Research Paper

Injectable OPF/graphene oxide hydrogels provide mechanical support and enhance cell electrical signaling after implantation into myocardial infarct

Jin Zhou[1*], Xiaoning Yang[1*], Wei Liu[1], Chunlan Wang[1], Yuan Shen[1], Fengzhi Zhang[1], Huimin Zhu[1], Hongji Sun[1], Jiayun Chen[3], Johnny Lam[2], Antonios G. Mikos[2], Changyong Wang[1✉]

1. Tissue Engineering Research Center, Academy of Military Medical Sciences and Department of Neural Engineering and Biological Interdisciplinary Studies, Institute of Military Cognition and Brain Sciences, Academy of Military Medical Sciences, Beijing, China.
2. Rice University, Department of Bioengineering, Houston, Texas, USA.
3. Collage of Life Science and Technology, Huazhong Agricultural University, Wuhan, Hubei, China.

*These authors contributed equally

✉ Corresponding author: Changyong Wang; 27 Taiping Road, Beijing 100850, PR China. wcy2000_te@yahoo.com

Abstract

After myocardial infarction (MI), the scar tissue contributes to ventricular dysfunction by electrically uncoupling viable cardiomyocytes in the infarct region. Injection of a conductive hydrogel could not only provide mechanical support to the infarcted region, but also synchronize contraction and restore ventricular function by electrically connecting isolated cardiomyocytes to intact tissue.

Methods: We created a conductive hydrogel by introducing graphene oxide (GO) nanoparticles into oligo(poly(ethylene glycol) fumarate) (OPF) hydrogels. The hydrogels were characterized by AFM and electrochemistry workstation. A rat model of myocardial infarction was used to investigate the ability of OPF/GO to improve cardiac electrical propagation in the injured heart *in vivo*. Echocardiography (ECHO) was used to evaluate heart function 4 weeks after MI. Ca^{2+} imaging was used to visualize beating cardiomyocytes (CMs). Immunofluorescence staining was used to visualize the expression of cardiac-specific markers.

Results: OPF/GO hydrogels had semiconductive properties that were lacking in pure OPF. In addition, the incorporation of GO into OPF hydrogels could improve cell attachment *in vitro*. Injection of OPF/GO 4 weeks after myocardial infarction in rats enhanced the Ca^{2+} signal conduction of cardiomyocytes in the infarcted region in comparison with PBS or OPF alone. Moreover, the injection of OPF/GO hydrogel into the infarct region enhanced the generation of cytoskeletal structure and intercalated disc assembly. Echocardiography analysis showed improvement in load-dependent ejection fraction/fractional shortening of heart function 4 weeks after injection.

Conclusions: We prepared a conductive hydrogel (OPF/GO) that provide mechanical support and biological conduction *in vitro* and *in vivo*. We found that injected OPF/GO hydrogels can provide mechanical support and electric connection between healthy myocardium and the cardiomyocytes in the scar *via* activating the canonical Wnt signal pathway, thus upregulating the generation of Cx43 and gap junction associated proteins. Injection of OPF/GO hydrogel maintained better heart function after myocardial infarction than the injection of a nonconductive polymer.

Key words: conduction, injectable biomaterials, myocardial infarction, remodeling

Introduction

Coronary heart disease is the leading cause of the rising incidence of heart failure worldwide, especially myocardial infarction (MI) [1-3]. The limited regenerative potential of the heart causes scar formation along the infarcted region following MI, leading to abnormal electric signal propagation and desynchronized cardiac contraction [4]. Injectable hydrogels have demonstrated great potential for

cardiac tissue repair and regeneration after MI. The injectable hydrogels can be injected alone or used as the delivery vehicle for therapeutic agents, including cells or growth factors, and can potentially provide mechanical and functional support to the infarcted region [5, 6].

Oligo(poly(ethylene glycol) fumarate) (OPF) is a macromer with alternating poly(ethylene glycol) (PEG) chains and fumarate groups, which allow for crosslinking and degradation through hydrolysis [7]. OPF hydrogels have been employed for the controlled delivery of growth factors and encapsulated cells for a variety of tissue engineering applications [8], especially in the field of osteochondral tissue regeneration. Previous findings have demonstrated that OPF hydrogels support the proliferation of encapsulated articular chondrocytes [8]. Additionally, previous *in vivo* investigations have shown the promise of OPF hydrogels as MSC delivery vehicles for osteochondral tissue regeneration [9]. These reports suggested that OPF hydrogel could provide mechanical support to the injured tissue and can be used to support tissue repair after MI. Previously, we have used OPF as a carrier of mouse embryonic stem cells (mESCs) for the treatment of MI. Four weeks after transplantation, OPF hydrogel significantly reduced the infarct size and collagen deposition and improved the cardiac function [10]. However, the implantation of OPF hydrogel alone, which is nonconductive, cannot restore impulse propagation to infarcted regions by electrically connecting isolated cardiomyocytes to intact tissue.

Graphene oxide (GO) is one of the widely investigated nanomaterials that has good electrical conductivity and appropriate mechanical properties. Previous studies have used GO as a scaffold material in tissue engineering applications, and have demonstrated the potential of GO to support cell adhesion, proliferation and differentiation [11-15]. For cardiac tissue engineering, previous studies have reported that GelMA, when blended with carbon-based nanoparticles such as multiwalled carbon nanotubes (CNTs) or GO, generates mechanically strong, electroconductive hydrogels that could support microvascular networks *in vivo* and support cardiomyocytes in a three-dimensional (3D) microenvironment [16-20].

In the present study, GO was incorporated into OPF hydrogels to generate an electrically conductive OPF/GO hydrogel. We found that electrically conductive OPF/GO composite hydrogels can enhance electric signal propagation in and around the infarcted region and improve cardiac repair when delivered to the heart tissue after MI.

Methods

Ethics statement

All animal care and experimental protocols complied with the Animal Management Rule of the Ministry of Health, People's Republic of China (Documentation No. 55, 2001). All procedures were approved by the Institutional Animal Care and Use Committee of Academy of Military Medical Sciences, Beijing, China.

OPF/GO hydrogel preparation and characterization

OPF and OPF/GO hydrogels were fabricated as described previously [9, 10]. Briefly, 0.16 g of OPF 10 K and 0.08 g of PEGDA were dissolved in 380 µL of phosphate buffered saline (PBS) or the GO dispersion (1.0 mg/mL) and incubated at 23 °C for 45 min to eliminate air bubbles. Thermal radical initiators, 74.9 µL of 300 mM N, N, N', N'-tetramethylethylenediamine (TEMED) solution (Sigma) and 74.9 µL of 300 mM ammonium persulfate (APS) solution (Sigma), were then added and incubated at 37 °C for 8 min for crosslinking. The electrical resistance of the hydrogel was detected by an electrochemistry workstation (CHI660D) (n=3/group).

Degradability was monitored as follows: OPF and OPF/GO hydrogels were prepared as described above [9, 10], except the polymer solutions were injected in Teflon molds (6 mm diameter by 0.5 mm thick) after mixing, and placed at 37 °C for 20 min afterwards. The resulting hydrogels were subject to degradation in PBS in 12-well tissue culture dishes at 37 °C on a shaker table shaking at 80 rpm. The PBS (2.5 mL/well) was completely changed every other day for the first week and the mass of the hydrogels was monitored every week. The mass remaining ratio of hydrogels (n=3) at each time point were represented as $w_d/w_i \times 100\%$, where w_i and w_d are the weight of the dried composite after fabrication prior to swelling, and the weight of the dried composite after swelling at each time point, respectively (n=3/group).

Ex vivo measurement of skeletomuscular signal propagation through OPF/GO

After euthanizing adult rats, rat leg skeletal muscle segments were explanted from the hind limbs. The muscles were cut in strips with a width of 10 mm and placed into a cell dish leaving a gap of 5 mm between two muscle pieces. This gap was filled with OPF or OPF/GO hydrogel, which acted as a bridge structure to connect two pieces of muscle tissue together. Voltage was then applied between two gel-connected muscle strips until contraction of both

pieces could be observed to determine the voltage threshold (n=3).

Biocompatibility of OPF/GO

Rat cardiac fibroblasts cells were isolated from 1-day-old neonatal Sprague-Dawley rats and seeded onto uncoated polystyrene dishes or those coated with OPF or OPF/GO at a concentration of 250 cells/mm² to assess cell attachment [13, 30, 37]. After 48 h, cells were stained with live & dead kit to analyze the cytocompatibility of OPF/GO.

To do immunocytochemistry, cultured cardiac fibroblasts were fixed in 4% paraformaldehyde for 30 min at room temperature. After fixation, cells were treated with 0.3% Triton X-100 for 30 min. Cells were then stained with vimentin primary antibody (Abcam) at 1: 200 dilution in blocking buffer for 24 h at 4 °C. Next, the sample was treated with secondary antibody (1: 200 dilution) in goat serum for 40 min. After washing with PBS, the sample was stained with DAPI (1: 200) diluted in PBS for 40 min at room temperature. The stained samples were then imaged with an inverted laser scanning confocal microscope (Leica SP5X MP, Germany). To assess the viability of cardiac fibroblasts on different materials, an MTT assay was performed according to the manufacturer's instructions. Briefly, a total of 1×10^4 cardiac fibroblasts were seeded on polystyrene, OPF or OPF/GO-coated 96 well surface, and grown for 48 h. Cardiac fibroblasts were incubated with MTT for 3 h at 37 °C, and cell viability was determined by measuring a test wavelength of OD 570 nm and a reference wavelength of 630 nm.

In vivo evaluation in rat infarct model

MI was induced in 27 male Sprague Dawley rats using an established model [19]. Briefly, the rats were anesthetized by injecting with 2% pentobarbital sodium into cavum abdominis. A left-sided open thoracotomy was performed, the heart was exposed, and the proximal left anterior descending artery (LAD) was ligated with 6-0 polypropylene. The rats were randomized into 3 groups and received separate peri-infarct intramyocardial injections of PBS (100 µL; n=7), OPF hydrogel (100 µL; n=10) or OPF/GO hydrogel (100 µL; n=10). Then, the thoracotomy was closed in multiple layers.

Echocardiography

Echocardiography (ECHO) was performed 4 weeks after hydrogel or PBS injection. Rats were anesthetized with 2% pentobarbital sodium. Standard transthoracic echocardiography was performed using the echocardiography system equipped with a 13 MHz linear ultrasonic transducer (15L8; Acuson Corporation, Mountain View, CA) in a phased array format. All analyses were performed by a single investigator who was blinded to the treatment groups (n=6/group).

Histological analysis and immuno-histochemistry

After 24 h, 1, 2, 3, and 4 weeks of injections, rats in all surgical groups were anesthetized, and the heart was exposed and arrested by apical injection of 1 mL 15% KCl. The hearts were explanted and fixed in 2% paraformaldehyde overnight and then were paraffin-embedded. The embedded tissues were serially sectioned at 3 µm in the LV transverse direction. Masson's trichrome staining was performed to measure infarct size. Hematoxylin and eosin staining was performed to measure the maintenance and distribution of OPF or OPF/GO hydrogel in the infarct region. Immunohistochemical staining was performed with antibodies against CD68 (Abcam), F-actin (Abcam), N-cadherin (Abcam), plakoglobin (Abcam), desmoplakin, alpha-smooth muscle actin (α-SMA, Abcam), connexin 43 (Cx43, Abcam) and α-actinin (Abcam). Moreover, the number of CD68+ cells was counted from 6 randomly selected fields at the infarcted zone under a magnification of 60×. Nuclei were stained with 4′, 6-diamidino-2-phenyindole (DAPI, Sigma). Morphometric analysis was performed to assess infarct and myocardial wall thickness. Infarct thickness was computed at each time point from the average spoke length. Infarct size was calculated as percentage of length of the infarcted endocardial circumference as previously described [21]. Capillaries were recognized as tubular structures positively stained for α-SMA as described in the literature [22].

Reverse transcription and quantitative polymerase chain reaction

4 weeks after injections, total RNA of the infarcted region was extracted using Trizol (Invitrogen). Total RNA was treated with DNase I (Invitrogen, CA, USA) to eliminate the genomic DNA carry over. DNase-treated RNA was reverse transcribed using high capacity cDNA kit (Toyobo). Real-time quantitative PCR (qPCR) was performed with Fast SYBR Green Master Mix (Toyobo). The corresponding primers were presented in **Table S1**.

Western blot analysis

Western blot analysis was carried out using lysates from infarct heart tissues 4 weeks after MI. The infarcted tissue and protein extract (TIANDZ, Beijing, China) were homogenized on ice. The supernatant was collected after centrifugation at 12000×g for 10-15 min. The extracted proteins were determined by using

BCA Protein Assay Kit (Thermo Scientific, USA). Equal amounts (50 µg) of denatured proteins were separated on 12% sodium dodecyl sulfate-poly-acrylamide gels and transferred to nitrocellulose membrane. The membranes were blocked with 5% defatted milk for 1 h and were incubated with these primary antibodies overnight at 4 °C. After being washed with Tris-base buffer, they were further incubated using appropriate secondary antibodies (goat anti-mouse or anti-rabbit IgG (Boster, Wuhan, China)) for 1 h at room temperature. The labeled proteins were visualized by enhanced chemi-luminescent reagent (Applygen, Beijing, China). GAPDH was used as an internal control to correct the variations of different samples.

Isolation of adult CMs

Adult CMs were isolated as described in literature [23], with minor modifications. Briefly, 4 weeks after injections, rats in all surgical groups were anesthetized. Hearts were removed and perfused via aortic cannulation with a constant flow of 3 mL/min in a Langendorff apparatus. Hearts were firstly perfused at 37 °C for 5 min with Tyrode's Solution containing 137 mM NaCl, 5.4 mM KCl, 0.5 mM MgCl$_2$, 5.0 mM D-glucose, 11.6 mM HEPES, and 1.8 mM CaCl$_2$ (pH 7.4). Then, the hearts were perfused for 3 min with the Tyrode's solution containing 130 mM NaCl, 5.4 mM KCl, 1.2 mM KH$_2$PO$_4$, 6.0 mM HEPES, and 10.0 mM D-glucose (pH 7.4), followed by digestion solution (0.8 mg/mL colleganse II) for 16 min. Hearts were then removed from the Langendorff apparatus while the tissues were gray and loosely connected. Desired areas (infarct zone) were then dissected in KB solution containing 50 mM L-glutamic acid, 30 mM KCl, 80 mM KOH, 30 mM KH$_2$PO$_4$, 20 mM taurine, 10 mM HEPES, 10 mM D-glucose, 3 mM MgSO$_4$, 0.5 mM EGTA (pH 7.4), mechanically dissociated, triturated, and resuspended in Tyrode's solution, and calcium was gradually reintroduced through a series of washes. For calcium transient measurements, cells were used on the same day as isolation.

Calcium-transient assessment

Calcium transients were assessed as previously described [23]. Briefly, isolated cardiomyocytes were loaded with Fluo-4 for 30 min at room temperature before measurements. The loading solution contained a 1:10 mixture of 5 mM Fluo-4 AM in dry DMSO, which was diluted 100-fold into extracellular Tyrode's solution containing suspended myocytes. After 30 min, the loading solution was extracted and added to the fresh Tyrode's solution. Then Fluo-4 fluorescence transients were recorded via live cell station.

Statistics

Statistical analyses were performed with Origin Pro 8.5 software. *p < 0.05 or **p < 0.01 was considered statistically significant.

Results

Characteristics of the OPF/GO hydrogel

To create an electrically conductive hydrogel, GO nanoparticles were incorporated into OPF hydrogel. A schematic of this study is shown in the graphical abstract. GO dispersion was introduced into OPF at 3 different concentrations (0.3 mg/mL, 0.6 mg/mL and 1.0 mg/mL GO/OPF) to form OPF/GO hydrogels (**Figure 1A**). To investigate the effects of GO nanoparticles on the local conductivity and morphology of the hybrid hydrogels, thin layers of OPF and OPF/GO hydrogels were coated on glass slides. AFM analysis was carried out to determine the morphology of the samples. As shown in **Figure 1C**, OPF sample showed a uniform topography, while the samples containing GO showed relatively rough surfaces, which was due to the presence of GO nanoparticles on the surfaces of the hydrogels. Additionally, the electrical conductivity of OPF/GO substrates was found to be significantly greater compared to that of OPF substrates (**Figure 1D**). The OPF/GO with the composite ratio of 1.0 mg/mL showed significantly higher conductivity (4.235×10^{-3} S/cm) than either 0.6 mg/mL OPF/GO, 0.3 mg/mL OPF/GO or pure OPF (0.905×10^{-3} S/cm).

To ascertain whether OPF/GO could support conduction between tissues more effectively than pure OPF *ex vivo*, we developed an assay for bioconductivity between isolated rat muscles. As shown in **Figure 1E**, pure OPF or OPF/GO hybrid hydrogels were injected into the gap between the tissues and allowed to crosslink. The hydrogels connected two pieces of muscle tissues together and acted as a bridge structure. One side of the muscle piece was then stimulated by applying an electrical voltage, while the beating or contraction of the other side muscle was checked and the applied voltage was increased until the muscles contracted. We observed a lower threshold for muscle tissue connected with OPF/GO (1.0 mg/mL) hybrid hydrogels (4.5±1.5 V, **Movie S1**) compared to the tissues linked with pure OPF hydrogel (**Figure 1F**, 10.5±1.5 V, **Movie S2**).

The prepared hydrogel degraded over time and the degradation ratio increased as culture progressed in all tested groups (**Figure 1B**). The mass remaining of OPF or OPF/GO was monitored every week until week 4. OPF had lost approximately 73% of its original weight whereas OPF/GO hydrogel with the composite ratio of 1.0 mg/mL lost only about 25% of
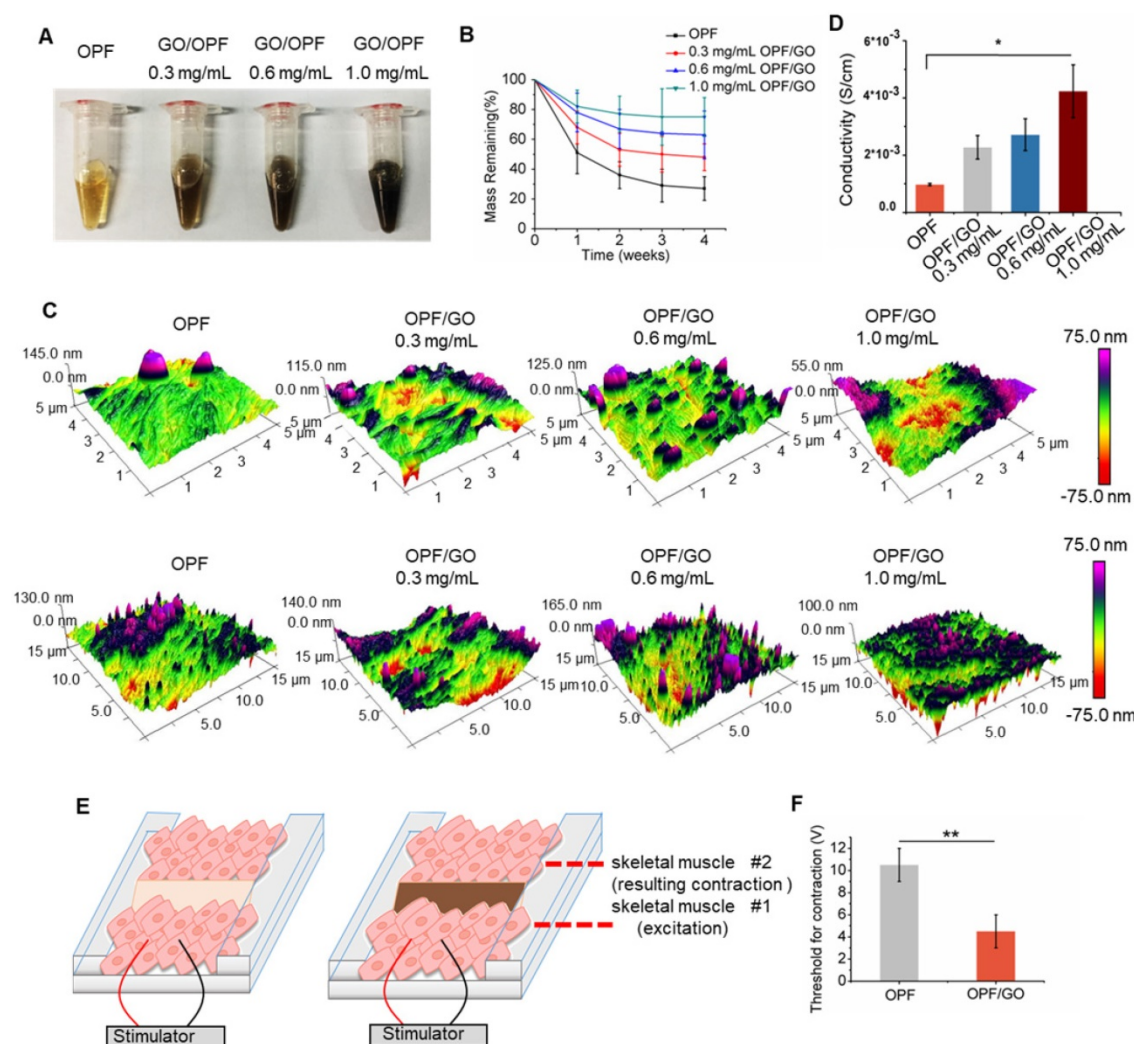
Figure 1. Synthesis and characterization of OPF/GO conductive hydrogel. (A) Photographs of OPF and OPF/GO hydrogels with various concentrations. **(B)** Degradation behavior of OPF and OPF/GO hydrogels (n=3/group). **(C)** Spatial topography of OPF and OPF/GO hydrogels measured by AFM. **(D)** Conductivity of OPF and OPF/GO with various concentrations (n=3/group). **(E)** A schematic illustration of the *ex vivo* setup used for measuring excitation threshold of muscle tissue. One muscle was electrically stimulated while the beating or contraction of the other muscle was monitored. **(F)** Excitation threshold of muscle tissue connected by pure OPF and OPF/GO hybrid gels, demonstrating that OPF/GO hybrid gels gave rise to the lowest excitation threshold, which was due to the conductivity of the OPF/GO hybrid gels (± standard deviation, n=3/group, *p < 0.05, or **p < 0.01).

its original weight, indicating degradation of both types of hydrogels and a higher degradation rate of OPF (n=3/group). Moreover, hydrogel degradation did not have significant effects on its electrophysiological properties (**Figure S1**).

Biocompatibility of OPF/GO Hydrogel *in vitro*

We investigated the biocompatibility of OPF/GO on cardiac fibroblasts, an important cell type in the heart after MI (**Figure S2A**). To demonstrate cell morphology and biomaterial attachment, rat fibroblasts were seeded on the surface of OPF- or OPF/GO hydrogel-coated wells and grown for 48 h (**Figure 2A** and **Figure S2B**). The effects of OPF/GO hydrogel on cardiac fibroblasts were investigated via live & dead staining. Compared with the cardiac fibroblasts seeded on OPF-coated surfaces, cells seeded on OPF/GO-coated surfaces maintained

excellent viability and few dead cells (red) could be observed on all OPF/GO hydrogels, indicating that the introduction of GO did not induce cytotoxicity even at GO concentrations up to 1.0 mg/mL (**Figure 2B**). In addition, the introduction of GO nanoparticles improved the poor cell adhesion on the OPF surface, which correlated with increasing GO concentration (**Figure 2C**). A similar effect was observed for the MTT assay (**Figure 2D**): the introduction of GO in the OPF hydrogel greatly enhanced cell adhesion, and the adhesion effects were correlated with GO concentration. No significant differences were observed in terms of cytotoxicity between OPF with 0.6 mg/mL GO and 1.0 mg/mL GO. On the other hand, the results in **Figure 1D** suggested that the electrical conductivity of OPF/GO hydrogel with the composite ratio of 1.0 mg/mL was significantly

higher than the rest. Therefore, OPF/GO with the composite ratio of 1.0 mg/mL was used in implantation research after MI.

In vivo biocompatibility evaluation

MI was induced in a rat model by occlusion of the left anterior descending coronary artery according to established laboratory procedures. Subsequently, 100 µL of injectable hybrid hydrogel was injected at three different sites in the peri-infarct regions of the heart. The rat models were divided into three groups and received PBS, OPF and OPF/GO injections, respectively. The rats were sacrificed at different time points (24 h, 1, 2, and 4 weeks) after injection to observe the histological responses to scaffolds using light microscopy.

As shown in **Figure S3A**, OPF/GO was still visible in H&E-stained heart sections of OPF/GO-treated hearts. The implant experiments suggested that the OPF/GO hydrogels could provide mechanical support to the infarcted region and interact directly with the infarcted tissue. 24 h after injection post MI, OPF or OPF/GO hydrogels were observed in cross sections of left ventricular tissue, which indicates direct interaction with the infarcted tissue at the early stage of MI. Along with partial degradation of OPF hydrogel with time after implantation, the biomaterial was gradually replaced by connective tissue and myofibroblasts. At 2 weeks and 4 weeks, only rare, weak pink-stained isolated islands of biomaterial were detected in the infarct area after OPF injection. However, in the OPF/GO-injected group, OPF/GO hydrogel was still visible and distributed continuously along the infarcted region at 4 weeks post MI (**Figure S3B**).

The inflammatory responses of injectable OPF/GO hydrogel in infarcted hearts

Considering the role of OPF and OPF/GO hydrogels in promoting macrophage recruitment and activation, we analyzed the infiltration of macrophages in the infarcted hearts. CD68+ cells were evaluated by immunofluorescence staining in the infarcted area of myocardial sections at 1 week after MI. No significant differences were observed in macrophage infiltration between PBS, OPF and OPF/GO-injected infarcts (**Figure 3A**). Compared to the PBS group, the ratio of CD68+ cells in the OPF- and OPF/GO-injected hearts was slightly increased (**Figure 3B**). Moreover, the recruitment of CD68+ cells was not significantly enhanced in or around the OPF/GO hydrogels in the infarcted region (**Figure 3C**).
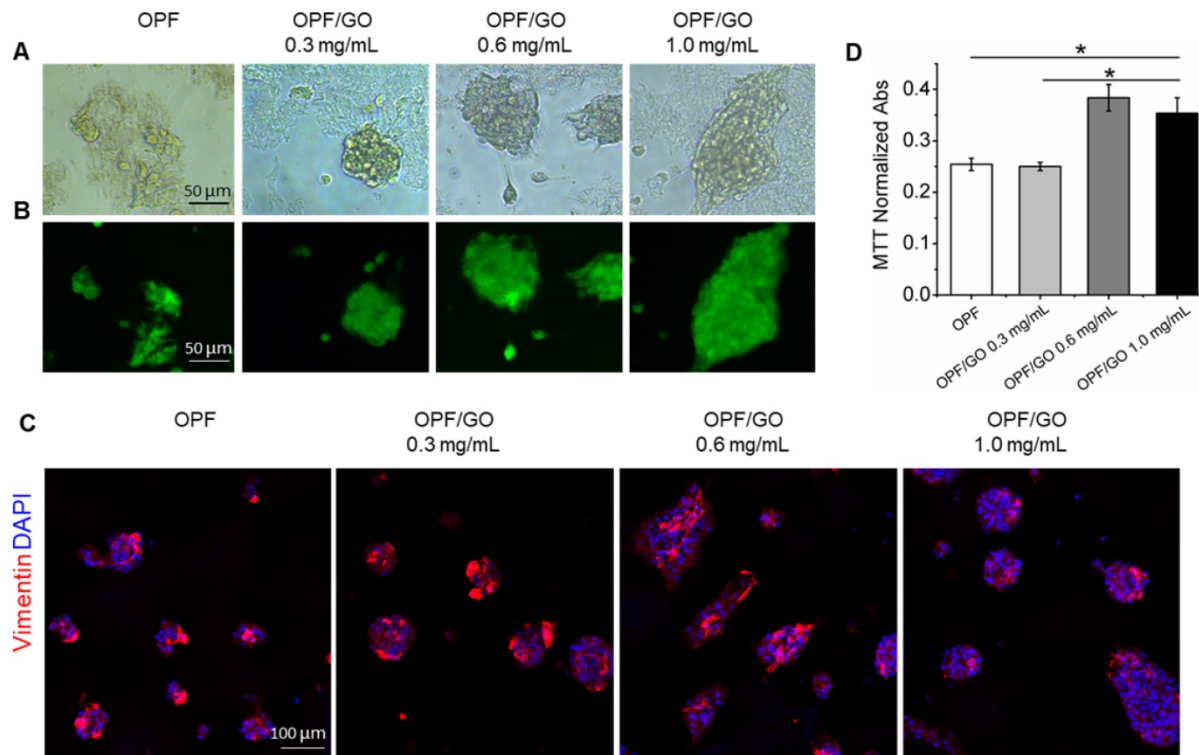

Figure 2. OPF/GO hydrogel supports cell growth without toxicity. (A) Representative morphological images of cardiac fibroblast cells cultured for 48 h on OPF- or OPF/GO-coated substrates. **(B)** Rat cardiac fibroblast cells were plated on the surfaces of wells coated with OPF or OPF/GO, grown for 48 h, and then stained with live & dead kit. **(C)** Immunofluorescence images of cardiac fibroblasts seeded on OPF- or OPF/GO-coated substrates (vimentin, red). **(D)** An MTT assay of cardiac fibroblasts cultured on the surface of pure OPF and different composite OPF/GO (0.3 mg/mL, 0.6 mg/mL, 1.0 mg/mL) (n=3, *P<0.05). MTT indicates 3-(4, 5-dimethylthiazol-2-yl)-2, 5-diphenyltetrazoliumbromide.
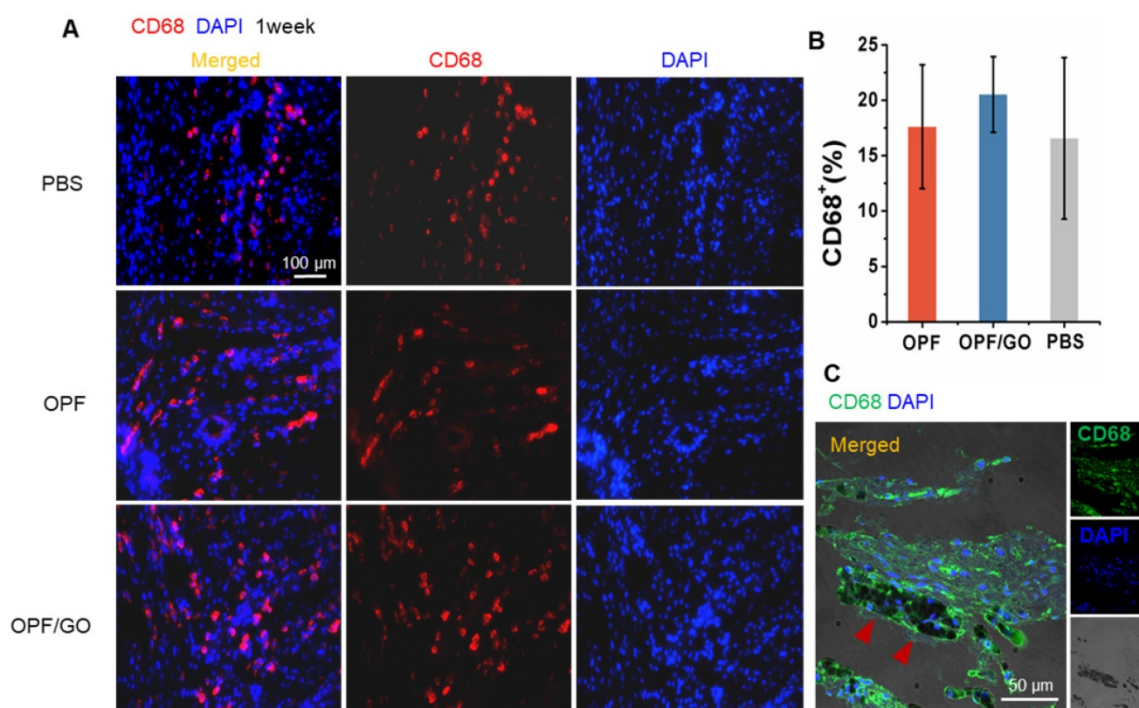
Figure 3. Effects of OPF and OPF/GO hydrogels on macrophage infiltration in infarcted hearts. (A) Representative fluorescence images show CD68-positive cells (left column, merged channel; middle column, CD68 (red); right column, DAPI (blue)) in PBS-, OPF-, and OPF/GO-injected hearts at 1 week post MI. **(B)** Quantification of CD68-positive cells of the corresponding images of (A). **(C)** CD68-positive signal is co-localized with the presence of OPF/GO hydrogel (CD68 (green), DAPI (blue)).

The injectable OPF/GO hydrogel enhanced cytoskeletal structure and intercalated disc assembly

As shown in **Figure 4A**, in the OPF/GO- and OPF-treated group, a cross-striated pattern can be obviously observed in the F-actin-positive area at 4 weeks post MI. Whereas in the PBS injected group, the pattern of the F-actin-positive area was weak and ambiguous (**Figure 4A-B**). In order to confirm if the enhanced generation of cytoskeletal structures was induced by the mechanical support of OPF and OPF/GO, we further explored the mechanism of the enhanced cytoskeletal structures and examined intercalated disc (ID) formation.

ID is important for cardiac integrity and function [24]. To determine whether the injection of OPF/GO had any influence on the assembly and formation of ID, ID-related proteins in the infarcted regions were characterized by immunofluorescence staining. Marker proteins including N-cadherin (NC) for adherens junctions, and plakoglobin (PG) and desmoplakin (DP) for desmosomes were examined 4 weeks post injection. As shown in **Figure 5A**, increases in localized structures were seen in the cell contact region, including the plaque pattern of N-C protein, stair-like distribution of PG protein (**Figure 5B**), and strand-like appearance of DP (**Figure 5C**). Meanwhile, NC, PG and DP showed larger linear

regions in the OPF/GO groups compared to those in the OPF and control groups, indicating the formation of better developed mechanical and gap junctions. To further quantify the ID-associated proteins, we quantified the ID-associated proteins by western blotting. The results suggested that ID-related protein expression in the OPF/GO group had significantly higher levels relative to those in the groups injected with OPF and PBS after 4 weeks (**Figure 5D**).

The injectable OPF/GO hydrogel promotes the expression of gap connexin proteins

Immunohistochemistry and histology of tissue sections revealed higher gap junction remodeling in the infarcted region of the OPF/GO-treated group than those in the OPF and PBS groups. Cx43 red fluorescence could be observed at the gap connexin region of the tissue by immunohistochemistry staining. As shown in **Figure S4A**, no significant differences were observed in the formation of gap junction-associated proteins between PBS-, OPF- and OPF/GO-injected infarcts 2 weeks after MI. The higher gap junction remodeling was observed obviously in the infarcted region of the OPF/GO hydrogel-treated group compared to those of the OPF- and PBS-treated groups at 3 weeks and 4 weeks (**Figure S4B** and **Figure 6A**). The expression levels of gap junction-associated markers Cx43, Cx40, Cx37 and Cx45 were analyzed by qPCR (**Figure 6B**). The

results were consistent with those of the immunohistochemistry analysis, where the mRNA expression level of gap connexin-associated genes in OPF/GO hydrogel was higher than that of OPF and PBS injection at 4 weeks post injection.

To further clarify the possible mechanism of the enhanced generation of connexin-associated proteins, we quantified the downstream signaling molecules of canonical Wnt signaling pathway by western blot (**Figure 6C**). Our data suggests that the introduction of GO improved the expression of total Akt. Although there were no significant differences in the expression of total GSK-3β among all experimental groups, the introduction of GO could improve the phosphorylation levels of GSK-3β (pGSK-3β) at 14 days post MI. Similarly, pGSK-3β could then induce β-catenin signaling and subsequently cause an increase in Cx43 expression (**Figure 6D**).
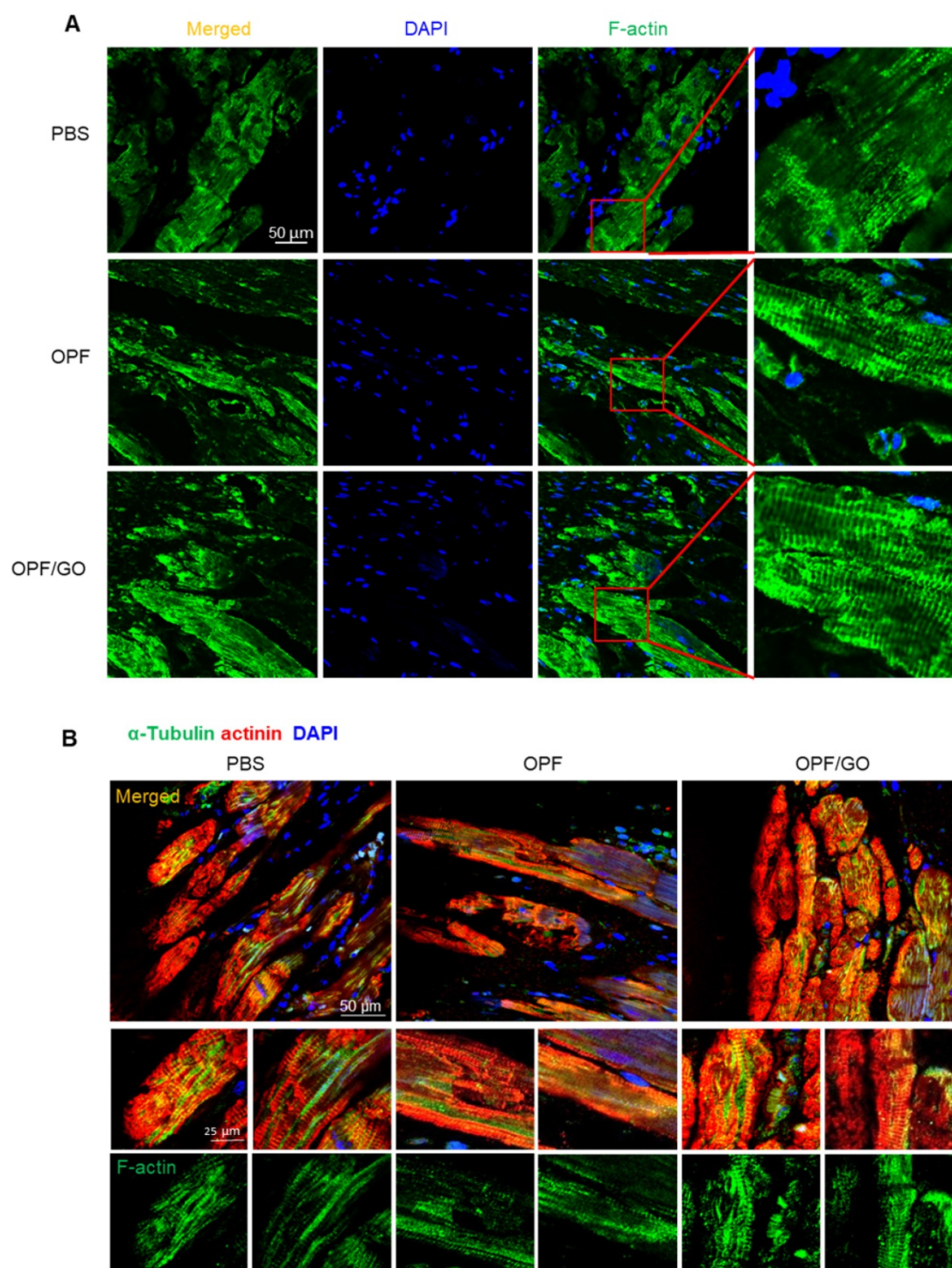

Figure 4. OPF/GO enhanced cytoskeletal structure 4 weeks after MI. (A) F-actin (green) in the infarcted areas of PBS-, OPF- and OPF/GO-treated groups at 4 weeks post MI (DAPI (blue)). **(B)** α-Tubulin (green) in the border zone cardiomyocytes (marked by actinin staining in red, DAPI (blue)).
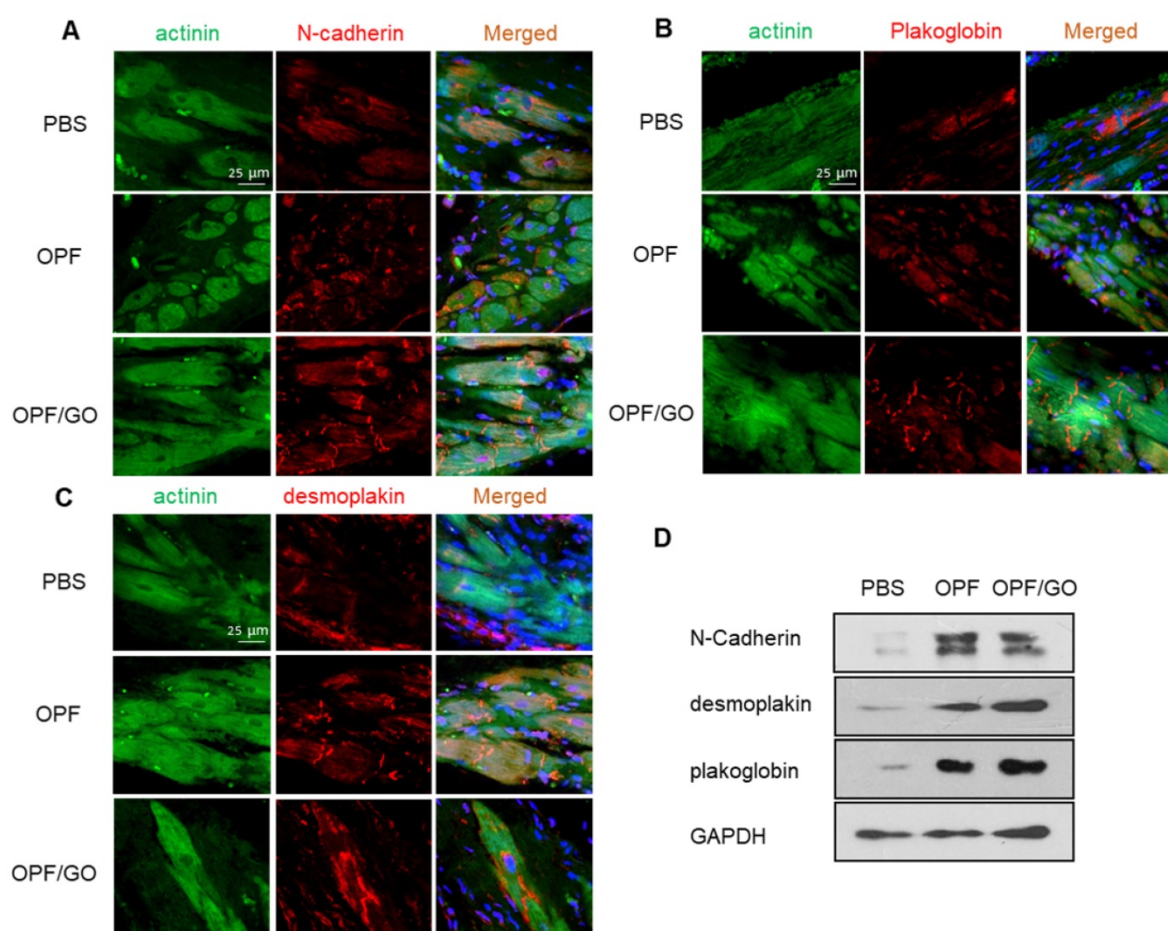
Figure 5. Immunofluorescence staining and quantification of ID-related proteins in the hearts of PBS-, OPF-, OPF/GO-injected groups at 4 weeks post MI. Marker proteins including N-cadherin (NC) for adherens junctions **(A)**, and plakoglobin (PG) **(B)** and desmoplakin (DP) **(C)** for desmosomes. **(D)** Western blot revealed the OPF/GO-injected group had significantly higher expression levels of NC, PG, and DP compared to the PBS- and OPF-injected groups.

Intramyocardial injection of the OPF/GO hydrogel improves cardiac function recovery after MI

Masson's Trichrome assay showed that there was extensive fibrous tissue formation in the border area of the PBS group, whereas little fibrosis was observed in the OPF/GO group. The control group receiving PBS injection had collagen zones occupying a large portion of the LV wall of the infarct site (**Figure 7A**), indicating the presence of widely spread scar tissue. In contrast, the animals injected with OPF/GO had visually more myocardial tissue at the infarct site. Consistent with this observation, LV wall thickness was significantly preserved (from 0.37±0.096 mm to 0.77±0.079 mm) in the OPF/GO injected group (**Figure 7B**); the infarct size was drastically decreased (from 50.7% to 31.7%; **Figure 7C**). These results suggest that the structural basis of the infarcted heart was effectively restored after OPF/GO injection.

The MI-damaged left ventricle undergoes progressive remodeling, leading to the deterioration of cardiac function [24]. Cardiac function was evaluated using echocardiography (ECHO) at 4 weeks post MI (**Figure 7D**). The results of echocardiography showed that LV ejection fraction (EF; **Figure 7E**) and fractional shortening (FS; **Figure 7F**), two important indicators for blood pumping function, were improved in both OPF and OPF/GO groups compared to PBS-injected rats. In particular, the hearts treated by OPF/GO show a significantly higher recovery of cardiac function than the OPF-treated group. Consistently, the OPF/GO group had a decrease in left ventricular end-diastolic dimension (LVEDD; **Figure 7G**) and left ventricular end-diastolic volume (LVESD; **Figure 7H**), indicating a functional improvement in ventricular filling. Together, these data proved that OPF/GO injection effectively promotes myocardial functional recovery after MI.

The injectable OPF/GO hydrogel promotes neovascularization

Angiogenesis restores blood supply to myocardium, facilitating cardiac function recovery [20]. We next investigated the effects of OPF/GO

injection on neovascularization after MI. The OPF/GO injection significantly increased the mRNA level of α-SMA (**Figure S5A**), vWF (**Figure S5B**) and VEGF (**Figure S5C**) at 4 weeks after LAD ligation, suggesting that OPF/GO injection may have an angiogenic effect. 4 weeks post injection, rats that received OPF/GO injections had a higher density of α-SMA-positive capillaries in the infarcted myocardium compared to both PBS- and OPF-treated

rats (**Figure S5D**). The undegraded OPF/GO hydrogel appeared to be distributed in the anterior wall and cell ingrowth was found inside or around the hydrogel area, with some regions of this tissue structure staining positively for α-SMA in higher magnification images (**Figure S5E**). These data suggested angiogenesis can be an outcome of gap junction enhancement.
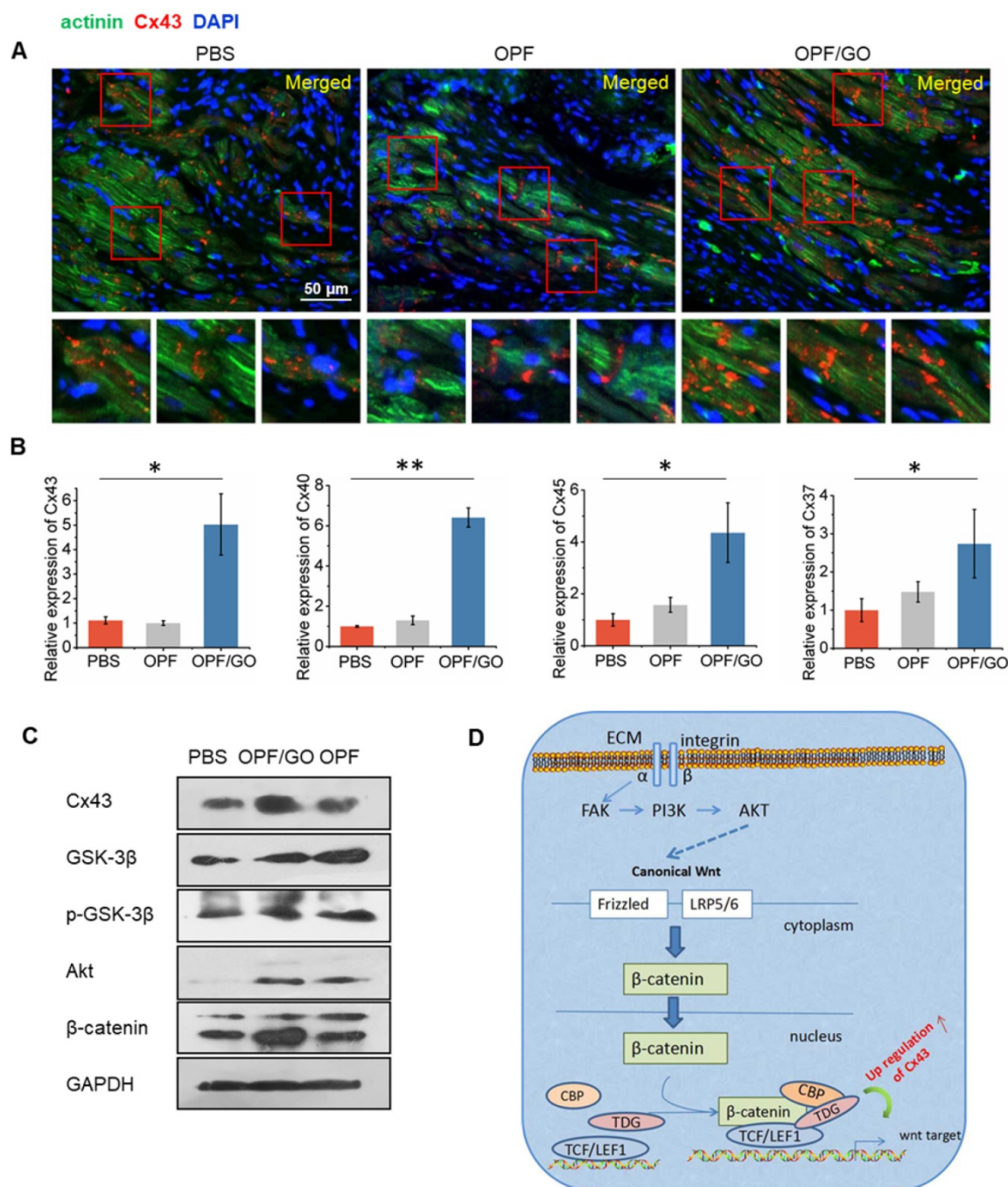

Figure 6. The formation of gap junction-associated proteins in the infarcted region. (A) Immunofluorescence staining revealed higher gap junction remodeling in the infarcted region of the OPF/GO hydrogel-treated group compared to the OPF- and PBS-treated groups. The highlighted areas are presented in the bottom images. **(B)** qPCR analysis of the expression levels of gap junction-associated markers Cx43, Cx40, Cx37 and Cx45. **(C)** Western blot revealed the downstream signaling molecules of canonical Wnt signaling pathway. **(D)** A schematic of the possible mechanisms.
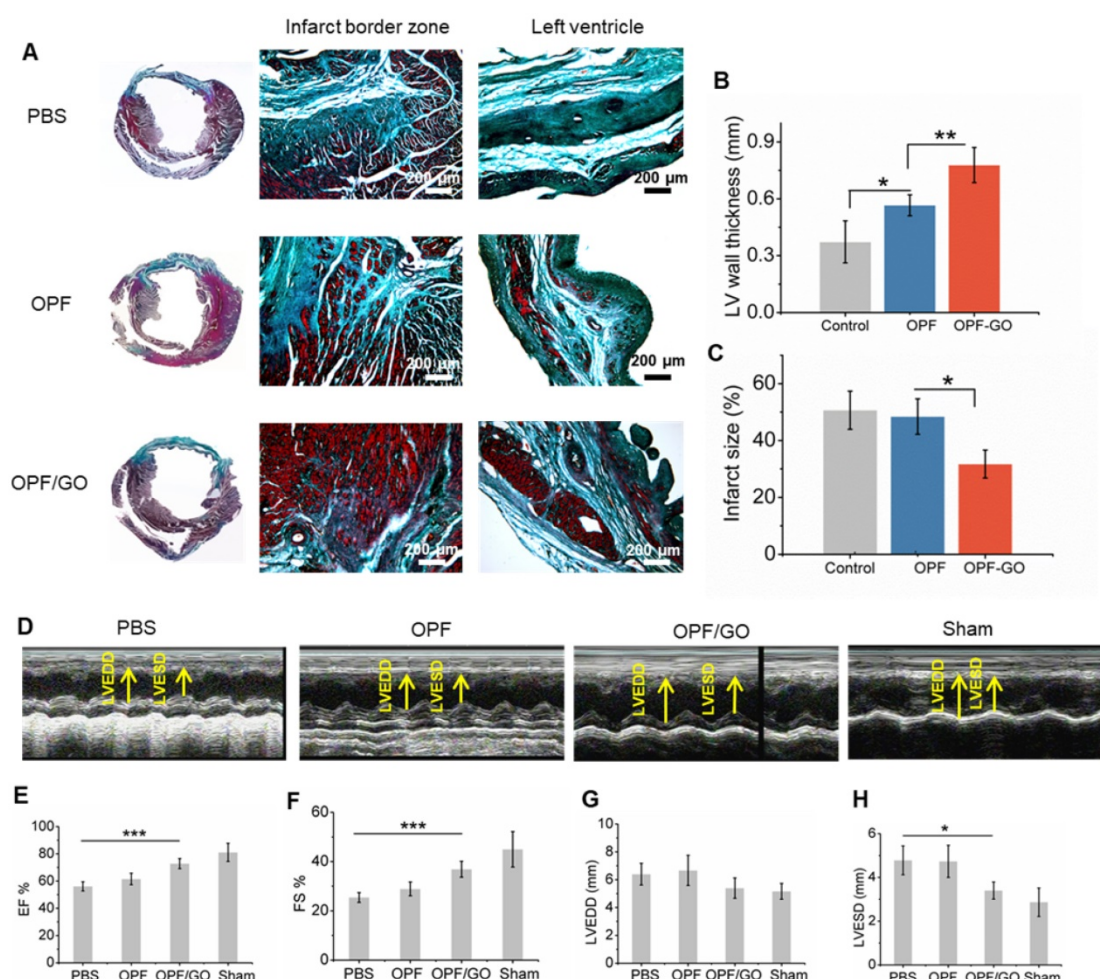
Figure 7. Masson's trichrome staining and echocardiographic measurements represent the effects of OPF/GO hydrogel on the morphology and myocardial functional recovery of infarcted hearts. (A) Masson trichrome staining of PBS-, OPF- or OPF/GO-injected heart 4 weeks post injection. Four weeks after injection, hearts were excised and left vetricle wall thickness **(B)** and infarct size **(C)** were measured. **(D)** Systolic ventricular function was improved after OPF/GO hydrogel injection into the border zone. Echocardiography (ECHO) was performed at 4 weeks post injection. Quantification of the parameters reflecting blood pumping function, including ejection fraction (EF) **(E)** and fractional shortening (FS) **(F)** 6 weeks after MI. Quantification of the parameters reflecting ventricular filling function, including left ventricular end-diastolic dimension (LVEDD) **(G)** and left ventricular end-systolic dimension (LVESD) **(H)**. Data is presented as mean ± standard deviation; *p < 0.05, or **p < 0.01 (n=6/group).

OPF/GO enhances calcium transient signal conduction of isolated cardiomyocytes in the infarcted area

To further investigate whether OPF/GO or OPF alone can promote electric conduction between cardiomyocytes and host tissue in the infarcted region, we isolated cardiomyocytes from the left ventricle of OPF/GO-, OPF- or PBS-injected rats 4 weeks after MI and labeled them with the Fluo-4 calcium dye. The Ca^{2+} fluctuations of cardiomyocytes can be observed (**Figure 8A-C**). In the OPF/GO-treated group, the isolated cardiomyocytes displayed rhythmic calcium transients and exhibited markedly high amplitudes of calcium transients (**Movie S3** and **Figure 8A**). While the cardiomyocytes isolated from the left ventricle of OPF-treated (**Movie S4** and **Figure 8B**) and PBS-treated (**Movie S5** and **Figure 8C**) rat MI models exhibited a uniform beating

frequency, the corresponding calcium transients amplitudes were lower than that of the OPF/GO-treated group. The results suggested that OPF/GO mediated the electrical conduction between cardiomyocytes and host tissue, thus promoting the intrinsic Ca^{2+} propagation of cardiomyocytes in the infarcted region.

Discussion

During the past 5 years, investigations into intramyocardial injection of bioengineered, chemically modified materials after MI have shown promising results [17]. For cardiac tissue engineering, electrical stimulation is important in assisting in the development of the tissue construct [2, 24]. Although traditional injectable hydrogels benefit cardiac function by providing structural support to the injured LV and enhancing myocardial regeneration, the contraction of the heart depends on the
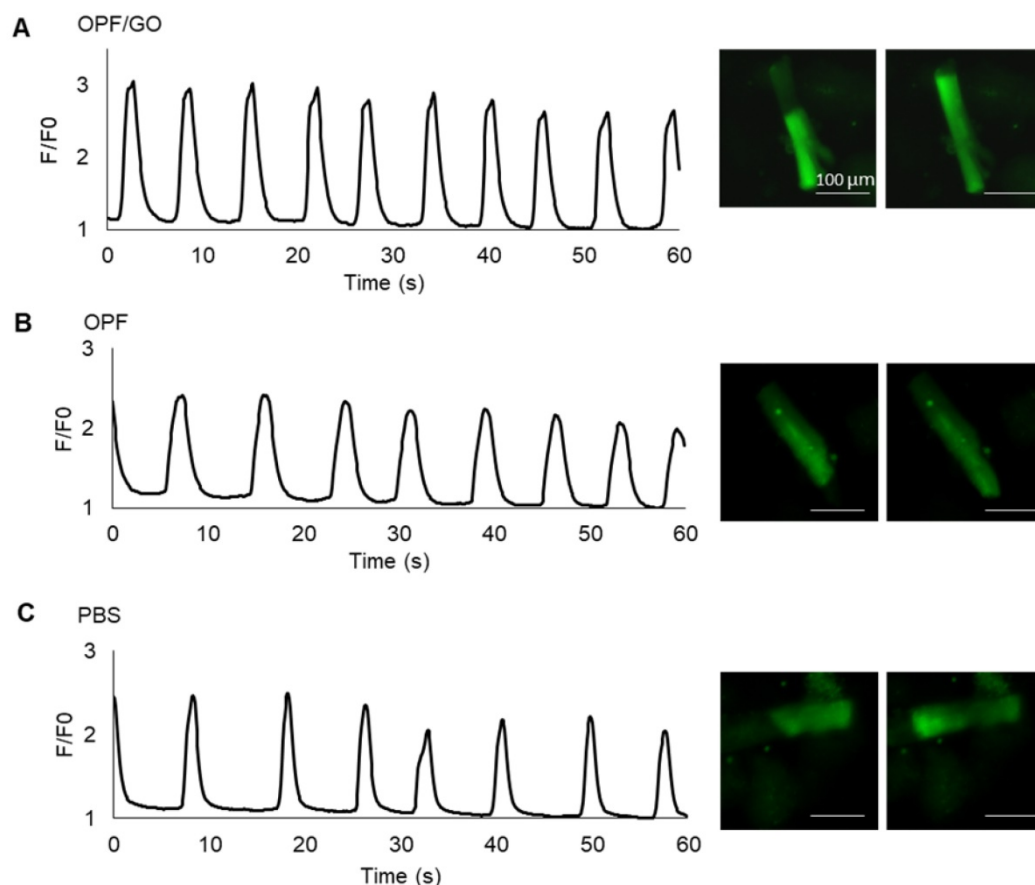
Figure 8. Ca^{2+} transients evaluation at 4 week after MI. Spontaneous Ca^{2+} transients of cardiomyocytes isolated from the left ventricle of OPF/GO- **(A)**, OPF- **(B)** or PBS- **(C)** injected rats four weeks after MI.

conduction of electric impulses through cardiac tissue, and conduction velocity is reduced in the infarct region following an MI [25, 26]. A conductive injectable hydrogel would potentially be able to synchronize ventricular contraction and substantially improve heart function post MI.

Conductive hydrogels, such as OPF/GO composite hydrogel, are biocompatible and have semiconductive properties that are capable of transmitting electric currents [27, 28]. The introduction of GO nanoparticles improved the poor cell adhesion of OPF, and is therefore suitable for tissue engineering applications. Our results demonstrated that OPF/GO injection after MI improved cardiac function in comparison with OPF- or PBS-treated groups. Although the mechanism of how OPF/GO improves cardiac function has not been fully investigated, the electric conductive property of GO is believed to contribute to the beneficial effects. GO is a single layer of sp2-hybridized carbon atoms tightly packed into a two-dimensional (2D) honeycomb lattice, and has emerged as a new class of nanomaterial for its mechanical strength and conductive properties [29]. Previous studies have confirmed GelMA/GO hydrogel can be microengineered to support microvascular networks *in vivo* and support cardiomyocytes in a three-dimensional (3D) microenvironment due to its strong mechanical and electroconductive properties [30]. In this study, we explored the therapeutic efficacy of OPF/GO hydrogel for tissue repair following MI. Calcium transients evaluation showed that the cardiomyocytes in the left ventricle in the OPF/GO-injected group displayed rhythmic calcium transients and exhibited markedly high amplitudes of Ca^{2+}. The results suggested that OPF/GO hydrogel could not only provide mechanical support to the infarcted region, but also enhance electro-physiological properties by electrically connecting isolated cardiomyocytes to intact tissue. The precise mechanisms for the observed effects of OPF/GO hydrogels in this study are not fully understood and deserve further investigations. There could be several reasons that account for the improvement of cardiac function by the OPF/GO injection post MI. Our H&E and immunofluorescence images suggest that GO developed close contacts with the cardiac tissue in or around the infarcted region, and one mechanism of GO/myocyte interaction may rely on the detection of irregular tight contacts between GO and membranes.

Such contacts are similar to that seen in cardiomyocytes cultured on carbon nanotubes, which promote growth and trigger spontaneous electrical activity [17, 31]. Furthermore, the electrically conductive networks formed by GO within OPF hydrogel are the key characteristics of GO/OPF that lead to improved cardiac cell adhesion, organization, and cell-cell interactions. GO, bridging the OPF hydrogel, provided additional pathways for direct electrical current flow and action potential propagation. A similar mechanism explained the electric signal propagation between cardiomyocytes through CNT networks [31].

Conclusion

Overall, graphene-based nanomaterials hold great promise for applications in cardiac tissue engineering. Most synthetic hydrogels used for tissue engineering are mechanically weak and lack conductive properties [33-36]. The addition of graphene-based nanoparticles imparted the required conductivity and surface properties to these hydrogel materials in several ways and further improved the microenvironment of the infarcted region [13-15, 32]. Therefore, these materials could be used in cardiac tissue engineering and injectable hydrogel-based therapeutic strategies.

Abbreviations

APS: ammonium persulfate; CMs: cardiomyocytes; CNTs: carbon nanotubes; Cx43: Connexin 43; DP: desmoplakin; ECHO: echocardiography; EF: ejection fraction; FS: fractional shortening; GO: graphene oxide; ID: intercalated disc; LAD: left anterior descending artery; LV: left ventricular; LVEDD: left ventricular end-diastolic dimension; LVESD: left ventricular end-diastolic volume; mESCs: mouse embryonic stem cells; MI: myocardial infarction; MTT: 3-(4, 5-dimethyl-thiazol-2-yl)-2, 5-diphenyltetrazoliumbromide; NC: N-cadherin; OPF: oligo(poly(ethylene glycol) fumarate); PBS: phosphate buffered saline; PEG: poly(ethylene glycol); PG: plakoglobin; TEMED: N, N, N', N'-tetramethylethylene- -diamine.

Supplementary Material

Supplementary figures and tables.
http://www.thno.org/v08p3317s1.pdf
Movie S1. http://www.thno.org/v08p3317s2.mp4
Movie S2. http://www.thno.org/v08p3317s3.mp4
Movie S3. http://www.thno.org/v08p3317s4.mp4
Movie S4. http://www.thno.org/v08p3317s5.mp4
Movie S5. http://www.thno.org/v08p3317s6.mp4

Competing Interests

The authors have declared that no competing interest exists.

References

1. Davis S, Norrving B. Organizational update: world stroke organization. Stroke. 2015; 46: e9-e10.
2. Hao T, Li J, Yao F, et al. Injectable fullerenol/alginate hydrogel for suppression of oxidative stress damage in brown adipose-derived stem cells and cardiac repair. ACS Nano. 2017; 11: 5474-5488.
3. Henning RJ, Khan A, Jimenez E. Chitosan hydrogels significantly limit left ventricular infarction and remodeling and preserve myocardial contractility. J Surg Res. 2016; 201: 490-497.
4. Palmer CR. Cardiac-resynchronization therapy in heart failure with a narrow QRS complex. New Engl J Med. 2013; 369: 1395-1405.
5. Russo V, Young S, Hamilton A, et al. Mesenchymal stem cell delivery strategies to promote cardiac regeneration following ischemic injury. Biomaterials. 2014; 35: 3956-3974.
6. Liu Z, Wang H, Wang Y, et al. The influence of chitosan hydrogel on stem cell engraftment, survival and homing in the ischemic myocardial microenvironment. Biomaterials. 2012; 33: 3093-3106.
7. Temenoff JS, Park H, Jabbari E, et al. Thermally cross-linked oligo(poly (ethylene glycol) fumarate) hydrogels support osteogenic differentiation of encapsulated marrow stromal cells *in vitro*. Biomacromolecules. 2004; 5: 5-10.
8. Lu S, Lam J, Trachtenberg JE, et al. Dual growth factor delivery from bilayered, biodegradable hydrogel composites for spatially-guided osteochondral tissue repair. Biomaterials. 2014; 35: 8829-8839.
9. Lam J, Lu S, Meretoja VV, et al. Generation of osteochondral tissue constructs with chondrogenically and osteogenically pre-differentiated mesenchymal stem cells encapsulated in bilayered hydrogels. Acta Biomater. 2014; 10: 1112-1123.
10. Xu G, Wang X, Deng C, et al. Injectable biodegradable hybrid hydrogels based on thiolated collagen and oligo(acryloyl carbonate)-poly(ethylene glycol)-oligo (acryloyl carbonate) copolymer for functional cardiac regeneration. Acta Biomater. 2014; 15: 55-64.
11. Kim J, Choi K S, Kim Y, et al. Bioactive effects of graphene oxide cell culture substratum on structure and function of human adipose-derived stem cells. J Biomed Mater Res A. 2013; 101: 3520-3530.
12. Sahni D, Jea A, Mata JA, et al. Biocompatibility of pristine graphene for neuronal interface. J Neuros-Pediatr. 2013; 11: 575-583.
13. Kim T, Kahng YH, Lee T, et al. Graphene films show stable cell attachment and biocompatibility with electrogenic primary cardiac cells. Mol Cells. 2013; 36: 577-82.
14. Park J, Park S, Ryu S, et al. Graphene–regulated cardiomyogenic differentiation process of mesenchymal stem cells by enhancing the expression of extracellular matrix proteins and cell signaling molecules. Adv Healthc Mater. 2014; 3: 176-181.
15. Lee TJ, Park S, Bhang SH, et al. Graphene enhances the cardiomyogenic differentiation of human embryonic stem cells. Biochem Bioph Res Co. 2014; 452: 174-180.
16. Su RS, Bae H, Cha JM, et al. Carbon nanotube reinforced hybrid microgels as scaffold materials for cell encapsulation. ACS Nano. 2012; 6: 362-72.
17. Shin SR, Jung SM, Zalabany M, et al. Carbon-nanotube-embedded hydrogel sheets for engineering cardiac constructs and bioactuators. ACS Nano. 2013; 7: 2369-80.
18. Ramón-Azcón J, Ahadian S, Estili M, et al. Dielectrophoretically Aligned Carbon nanotubes to control electrical and mechanical properties of hydrogels to fabricate contractile muscle myofibers. Adv Mater. 2013; 25: 4028-4034.

19. Shin SR, Aghaei-Ghareh-Bolagh B, Dang TT, et al. Cell-laden Microengineered and Mechanically Tunable hybrid hydrogels of gelatin and graphene oxide. Adv Mater. 2013; 25: 6385-91.
20. Zhou J, Chen J, Sun HY, et al. Engineering the heart: evaluation of conductive nanomaterials for improving implant integration and cardiac function. Sci Rep. 2014; 4: 3733-43.
21. Pfeffer MA, Pfeffer JM, Fishbein MC, et al. Myocardial infarct size and ventricular function in rats. Circ Res. 1979; 44: 503-12.
22. Fujimoto KL, Ma Z, Nelson DM, et al. Synthesis, characterization and therapeutic efficacy of a biodegradable, thermoresponsive hydrogel designed for application in chronic infarcted myocardium. Biomaterials. 2009; 30: 4357-68.
23. Qian L, Huang Y, Spencer CI, et al. *In vivo* reprogramming of murine cardiac fibroblasts into induced cardiomyocytes. Nature. 2012; 485: 593-8.
24. Sun H, Lü S, Jiang XX, et al. Carbon nanotubes enhance intercalated disc assembly in cardiac myocytes via the $\beta 1$-integrin-mediated signaling pathway. Biomaterials. 2015; 55: 84-95.
25. Wang Z, Zhang Y, Zhang J, et al. Exploring natural silk protein sericin for regenerative medicine: an injectable, photoluminescent, cell-adhesive 3D hydrogel. Sci Rep. 2014; 4: 7064-74.
26. Bilchick KC, Kuruvilla S, Hamirani YS, et al. Impact of mechanical activation, scar, and electrical timing on cardiac resynchronization therapy response and clinical outcomes. J Am Coll Cardiol. 2014; 63: 1657-1666.
27. Yang J, Goeun C, Yang S, et al. Polypyrrole-incorporated conductive hyaluronic acid hydrogels. Biomaterials Research. 2016; 20: 31-37.
28. Dong R, Zhao X, Guo B, et al. Self-healing conductive injectable hydrogels with anti-bacterial activity as cell delivery carrier for cardiac cell therapy. ACS Appl Mater Inter. 2016; 8: 17138-17150.
29. Xiang Q, Yu J, Jaroniec M. Graphene-based semiconductor photocatalysts. Chem Soc Rev. 2012; 41: 782-796.
30. Annabi N, Shin SR, Tamayol A, et al. Highly elastic and conductive human-based protein hybrid hydrogels. Adv Mater. 2016; 28: 40-49.
31. Martinelli V, Cellot G, Toma FM, et al. Carbon nanotubes promote growth and spontaneous electrical activity in cultured cardiac myocytes. Nano Lett. 2012; 12: 1831-1838.
32. Park J, Kim B, Han J, et al. Graphene oxide flakes as a cellular adhesive: prevention of reactive oxygen species mediated death of implanted cells for cardiac repair. ACS Nano. 2015; 9: 4987-99.
33. Wassenaar JW, Gaetani R, Garcia JJ, et al. Evidence for mechanisms underlying the functional benefits of a myocardial matrix hydrogel for post-MI Treatment. J Am Coll Cardiol. 2016; 67: 1074-1086.
34. Xu G, Wang X, Deng C, et al. Injectable biodegradable hybrid hydrogels based on thiolated collagen and oligo(acryloyl carbonate)-poly(ethylene glycol)-oligo (acryloyl carbonate) copolymer for functional cardiac regeneration. Acta Biomater. 2014; 15: 55-64.
35. Dorsey SM. MRI evaluation of injectable hyaluronic acid hydrogel therapy to attenuate myocardial infarct remodeling. Antitrust Law J. 2015; 57: xxvii-xxxvii.
36. Wang W, Liang S, Liu WG. Opinion on the recent development of injectable biomaterials for treating myocardial infarction. Sci China Technol Sc. 2017; 60: 1278-1280.
37. Shin H, Zygourakis K, Farach-Carson MC, et al. Attachment, proliferation, and migration of marrow stromal osteoblasts cultured on biomimetic hydrogels modified with an osteopontin-derived peptide. Biomaterials. 2004; 25: 895-906.